Protein-Protein Ratchets: Stochastic Simulation and Application to Processive Enzymes

Charles J. Brokaw
Division of Biology, California Institute of Technology, Pasadena, California 91125 USA

ABSTRACT Interaction between a protein and a series of binding sites on a cytoskeletal substrate can create a resistance, or "protein friction," as the protein is moved along the substrate. If attachment and detachment rates are specified asymmetrically, this resistance can depend on the direction of movement, and the binding interaction acts as a ratchet. Stochastic computer simulations have been used to examine this type of protein-protein interaction. The performance of a protein-protein ratchet in the piconewton and nanometer range is significantly limited by thermal fluctuations, which in experimental measurements with single molecules are evident as Brownian motion. Simulations with a two-component model combining a conventional motor enzyme model with a protein-protein ratchet confirm previous suggestions that the processive movement of a single motor enzyme molecule against a load, as seen in experiments with inner arm dynein molecules, might be made possible by an accessory protein interaction that prevents backward slippage. When this accessory protein interaction is defined so that it acts as a ratchet, backward slippage can be prevented with minimal interference with forward progression.

INTRODUCTION

A ratchet is a mechanical device that restricts movement in one direction and allows movement in the opposite direction. Similar to an electrical diode that rectifies an alternating voltage, it might rectify an alternating force to generate a net movement in one direction. The possibility that a microscopic ratchet could rectify random thermal fluctuations (Brownian motion) to generate unidirectional movement was discussed by Feynman et al. (1966), who explained that this would be impossible unless there was an energy source such as a temperature difference. Several recent authors have explored the ways in which energy provided by a chemical reaction, such as dephosphorylation of adenosine 5′-triphosphate (ATP), could be applied to a molecular-level ratchet to produce molecular fluxes and movements (Vale and Oosawa, 1990; Astumian and Bier, 1996; Julicher et al., 1997). Such models have been suggested as alternatives to mechanisms relying on energy-driven conformational changes within transport or motor enzymes. Much of this exploration has assumed the existence of a molecular level ratchet, without supporting detail. Motor enzyme models containing asymmetric strain dependencies of rates for some steps in the mechanochemical cycle have also been characterized as ratchet models (Cordova et al., 1992; Smith, 1998a).

This paper examines whether asymmetric specification of the binding interaction between a protein and a cytoskeletal polymer such as a microtubule can create a useful ratchet. This examination was stimulated by recent observations of processive movement against a load by single motor enzyme molecules. A motor molecule that moves against an external load by conventional attachment-detachment cycles is expected to be pushed backward rapidly by the load when it is detached. Some other component of the molecule might resist this backward movement, but it might be advantageous for this component to have ratchet-like properties, to minimize its resistance to forward movement of the motor.

Received for publication 23 January 2001 and in final form 25 May 2001.

Address reprint requests to Dr. Charles J. Brokaw, Kerckhoff Marine Laboratory, 101 Dahlia St., Corona del Mar, CA 92625. Tel.: 626-395-6294; Fax: 949-675-1837; E-mail: brokawc@its.caltech.edu.

0006-3495/01/09/1333/12 $2.00

METHODS

The models in this paper were examined by computer simulations using stochastic (Monte Carlo) methods developed previously for modeling motor enzyme function (Brokaw, 1976, 1995, 1999; Pate and Cooke, 1991). The computer simulation program is a slightly modified version of a program used for modeling dynein function in flagella (Brokaw, 1999) and is available as a Macintosh application at www.its.caltech.edu/~brokawc/software.html. The most important modification is the inclusion of random thermal forces that produce Brownian motion of the molecule or its substrate. This modification is required for modeling the behavior of single molecules in either of two commonly used experimental situations. One situation assumes that a protein molecule attached to a fixed support interacts with a moving substrate, such as a microtubule, that is free to move only in the direction parallel to its length. The other situation assumes that a protein molecule is attached to a bead held in an optical trap and is interacting with a microtubule that is rigidly attached to a fixed support such as a microscope slide. Fortunately, it is reasonable to assume that the viscous resistances on the microtubule or the bead in these two experimental situations are similar and use a value of $\zeta = 10^{-5}$ pN s nm^{-1} in both cases (Brokaw, 2000). Both situations can be described by an overdamped Langevin equation, but they have different sign conventions. This equation is for the moving microtubule situation. For numerical work, the discrete form is:

$$\frac{\zeta \Delta s}{\Delta t} = F_{\text{protein}} - F_{\text{load}} + F_{\text{random}} \quad (1)$$

The internal force generated by a protein, $F_{\text{protein}} = k_F\,(x(t) - \Delta s)$, is determined by a linear elastic constant k_F and by internal strain $x(t)$. These values depend on the state of the protein, and k_F will be 0 when the protein

is detached from the substrate microtubule. In experiments with optical traps, the load force $F_{load} = k_{load}(s(t) + \Delta s)$ is determined by the trap stiffness k_{load} and the shear distance $s(t)$ from the null position of the trap. These expressions for F_{load} and $F_{protein}$ use implicit integration so that the elastic terms are in balance at $t + \Delta t$ even if ζ and F_{random} are small (Pate and Cooke, 1991). The shear s is a measure of the overall movement of the microtubule or bead, and $\Delta x = -\Delta s$ unless there is a change in the attachment of the protein. This allows Eq. 1 to be solved for Δs, which is then used to calculate $x(t+\Delta t)$ and $s(t+\Delta t)$. The F_{random} is obtained by taking a random deviate from a normal (Gaussian) distribution (Press et al., 1986) and multiplying by a scaling factor of $(2\zeta k_B T/\Delta t + k_B T k_{total})^{1/2}$. In this case, k_{total} is the sum of k_F and k_{load}, and $k_B T$ is the product of Boltzmann's constant and absolute temperature. The first term in the scaling factor (Smith, 1998b; Keller and Bustamente, 2000) is augmented by a second term required for the implicit solution of Eq. 1 to obtain the correct value of mean square deviation $\langle s^2 \rangle = k_B T/k_{total}$ even at small values of ζ. Validation of this method is discussed in Brokaw (2000).

The models consider the interaction of individual protein molecules with a series of sites on a cytoskeletal substrate. This interaction involves several attached and detached states of the protein. The kinetic equations governing transitions between these states are integrated to calculate transition probabilities for a small time interval, Δt (Brokaw, 1995, 1999). These probabilities are tabulated at 0.2-nm intervals from $x = -30$ to $+30$ nm, and linear interpolation is used at intermediate x values. Given the state of the protein at time t, these transition probabilities are compared with a random variable to determine the state of the protein at time $t + \Delta t$. The updated state of the protein is then used to obtain its strain $x(t)$ for calculation of Δs by Eq. 1. The process is then repeated, using transition probabilities appropriate for the new position of the protein. Because some of the transition probabilities depend on the distance x between a protein and a binding site, the time interval Δt must be small enough to justify the approximation that the transition probabilities are constant during Δt. For this paper a value of $\Delta t = 10^{-7}$ s has been used; with this value and $\zeta = 10^{-5}$ pN s nm^{-1}, the root mean square displacement during Δt resulting from random thermal force fluctuations when the protein is detached is 0.28 nm. Some results were recalculated with larger values of Δt. With $\Delta t = 10^{-6}$ s, recalculation of Fig. 2 *B* gave results that were indistinguishable from those shown in Fig. 2 *B*. Recalculation with $\Delta t = 10^{-5}$ s gave results that were qualitatively the same, but quantitatively slightly different. Recalculation of Fig. 8 *A* with either $\Delta t = 10^{-6}$ s or $\Delta t = 10^{-5}$ s gave results that were indistinguishable from the result shown.

Some models allow an attachment site to be within range of more than one binding molecule. In such cases, an interference check is required to disallow multiple attachments to the same site. This was carried out by checking for previous occupancy before allowing an attachment. If a site is already occupied, a new random number is obtained and compared with the transition probabilities, and this is repeated until an allowable result is obtained. To prevent directional bias when this checking is necessary, the direction of processing the array of molecules is reversed at each time step.

Values reported at fixed loads at 0.5 mM ATP are mean velocities from three computations, for 0.5 s with single motors or 0.05 s with ensembles of 100 motors. Variations within a set of three computations were similar to those illustrated in Fig. 2. Results for movement against an elastic load, as in Fig. 8 *A*, are representative of at least 3 separate computations for each situation.

RESULTS

Basic model for interaction of a protein with a cytoskeletal substrate

The cytoskeletal substrate is assumed to be a linear polymer with binding sites at regular intervals, d, along its length. The position of the protein molecule, relative to a binding site, is measured by the variable x. If the protein is attached at a binding site, x measures strain, but the localization of that strain within the protein molecule is not specified. The protein is considered to be located at the binding site when the strain is 0. At a static equilibrium, a load force, $F(x)$, must be applied to an attached protein to maintain it in a strained position. The convention used is that a positive value of x must be maintained by a positive load.

Attachment and detachment of the protein are considered by defining a detached state 2, an attached state 3, an attachment rate function $k_{23}(x)$ and a detachment rate function $k_{32}(x)$. This numbering convention is used for consistency with the motor enzyme models of Brokaw (1999) and the related motor enzyme model used later in this paper (Fig. 7). The attachment and detachment rates must be related (Hill, 1974) as

$$k_{32}(x) = k_{23}(x)\exp(A(x)/k_B T), \tag{2}$$

where $A(x)$ is a potential function such that

$$F(x) = dA(x)/dx. \tag{3}$$

In Eq. 2, $k_B T$ represents the product of Boltzmann's constant and absolute temperature, and in this work is given a nominal value of 4.00 pN nm. The model represented by Eqs. 2 and 3 assumes that the detached state is a state where the detached protein remains in a favorable position for reattachment. It is appropriate for cases where motor enzymes are held in a cytoskeletal array, such as the array of actin and myosin filaments in muscle or the outer doublet microtubule array in an axoneme. It may not be appropriate for situations with individual motor enzyme molecules where a "just-detached" motor may remain close to a site for a short time, and have a higher reattachment probability, before it diffuses away and its attachment rate depends on the solution concentration of the motors. The modeling in this paper assumes that movement between the protein and the substrate microtubule occurs only in a direction parallel to the length of the microtubule.

Mechanical properties of the model defined by Eqs. 2 and 3 were examined in detail by Schoenberg (1985) using analytical methods and by Brokaw (1995) using numerical simulation. This earlier work calculated the resisting force, or "protein friction" (Tawada and Sekimoto, 1991) developed when an ensemble of proteins is moved past an array of sites at a predetermined velocity. When thinking about experiments with single motor enzyme molecules, it is more appropriate to calculate velocity when loaded with an applied force, and it is essential to include the Brownian motion of the microtubule resulting from random thermal forces.

For the simplest case, with a symmetric model, four specifications (a, b, c, d) are needed:

a) The spacing between sites, $d = 8$ nm. A microtubule, the substrate for kinesin and dynein motors, is considered to fit this description. This is an oversimplification, because a

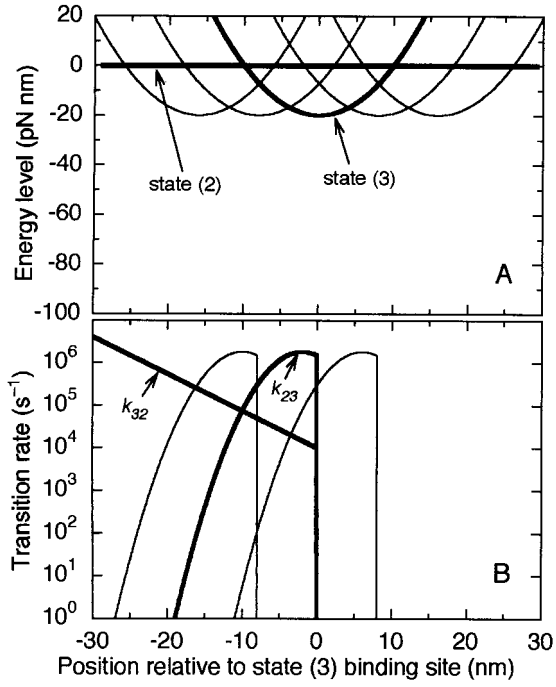

FIGURE 1 *A* shows energy levels for a simple interaction between a protein and a series of binding sites at 8-nm intervals. The detached state is state 2. The principal attachment is in state 3, and the model includes the possibility of attachments to two sites on each side of the state 3 site at $x = 0$. The linear elastic constant for the attached state, k_F, is 0.4 pN nm^{-1}. The energy scale is extended to -100 pN nm to emphasize comparison with motor enzyme models where the energy change in one mechanochemical cycle is up to 100 pN nm (see Fig. 7). Some of the rate functions are shown in *B*, for the asymmetric rates case where the k_{23} and k_{32} rates are 0 for $x > 0$.

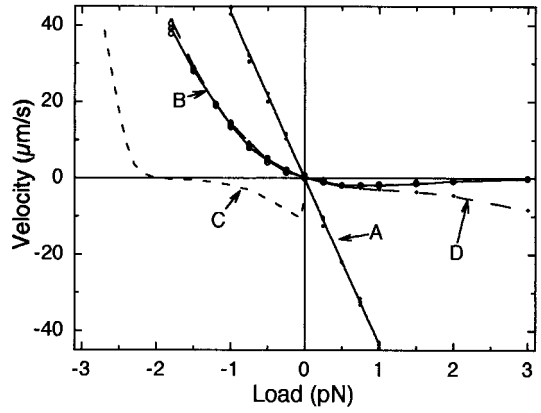

FIGURE 2 Velocity when a single protein is interacting with sites at 8-nm intervals as a function of applied load. *A* is for symmetric interaction, with Brownian motion of the microtubule included; the regression line has a slope corresponding to a resistance of 2.3×10^{-5} pN s nm^{-1}. *B* and *C* show results obtained with asymmetric interaction when attachment and detachment rates are 0 for $x > 0$. *D* shows results obtained with a weaker version of the asymmetric rate model, with attachment and detachment rates reduced by a factor of 0.01 for $x > 0$. Brownian motion was included in *B* and *D*, but not in *C*. Velocity was averaged over 0.5 s, after a 0.5 startup period to eliminate starting transients. Three computations were performed at each value of load, and shown by *small, solid points* in *A*, and by *open circles* in *B*. The *solid line* in *B* and the *dashed lines* in *C* and *D* connect points that are the average of the three computations at each load value. The sign convention is that a positive velocity is in the direction of $-x$ (as defined in Figs. 1 *A* and 7), and corresponds to the usual direction of movement produced by a motor enzyme working against a positive applied load. Velocity is placed on the ordinate because it is the dependent variable, resulting from the computations. With these conventions, a motor enzyme would normally work with positive values of velocity and load, in the upper right quadrant, and would only enter the lower right quadrant (backward movement) when the load exceeds the isometric force. Here, for a purely resistive interaction, any positive load causes a negative velocity (*lower right quadrant*), and a negative load produces a positive velocity (*upper left quadrant*).

microtubule is constructed of parallel protofilaments that are staggered in a manner that might present binding sites at intervals other than the basic periodicity of the protofilament. Observations of microtubule rotation by inner arm dyneins indicate that these dyneins do not track precisely along a single protofilament (Vale and Toyoshima, 1988; Kagami and Kamiya, 1992).

b) The free energy difference between the attached state 3 and the detached state 2 when $x = 0$ is $\Delta E_{23} = -20$ pN nm, or $-5\ k_BT$.

c) The force is a linear function of strain: $F(x) = k_F x$, and $A(x) = \Delta E_{23} + 0.5 k_F x^2$. A reasonable value of k_F is 0.4 pN nm^{-1}.

Specifications a, b, and c are illustrated by the free energy diagram in Fig. 1 *A*.

d) $k_{32} = 10{,}000$ s^{-1} at $x = 0$. This detachment rate is increased by strain as found with experimental measurements of force-induced protein dissociation (Nishizaka et al., 2000; Strunz et al., 2000), so that $k_{32}(x) = k_{32}(0) \exp(a|F(x)|/k_BT)$. The constant a is given a value of 2.0 nm. $k_{23}(x)$ can then be calculated from Eq. 2. Rates for attachments to and detachments from two additional sites at 8-nm intervals on each side of $x = 0$ are also determined and used in the computation of transition probabilities.

Fig. 2 (*curve A*) shows results from computer simulations that calculate the velocity of movement that would result when a constant force is applied to a microtubule that is interacting with a single protein. For these computations, F_{load} in Eq. 1 is given a constant value, independent of position. At each load value, three computations of the average velocity for a period of 0.5 s (after an initial 0.5 s to eliminate any starting transients) were performed. The results show a nearly linear relationship between velocity and force, with a slope corresponding to a resistance of 2.3×10^{-5} pN s nm^{-1}. After subtracting the resistance of 1.0×10^{-5} pN s nm^{-1} contributed by the viscous load on the microtubule, a resistance of 1.3×10^{-5} pN s nm^{-1} is the result of the protein-protein interaction.

Another computation, not shown, was carried out using a constant value of $k_{32} = 8000$ s^{-1}, independent of x. These results also show a nearly linear relationship between velocity and force, corresponding to a resistance of 5.5×10^{-5} pN s nm^{-1}. After subtracting the viscous resistance of

1.0×10^{-5} pN s nm^{-1}, a resistance of 4.5×10^{-5} pN s nm^{-1} is the result of the protein-protein interaction. This can be compared with the analytical result that can be obtained with constant k_{32} (Case I of Schoenberg, 1985), which gives a resistance equal to $k_F/k_{32} = 5 \times 10^{-5}$ pN s nm^{-1} times the fraction of time in the attached state, which in this case is close to 1.0.

Interaction with asymmetric attachment and detachment rates

Fig. 2 (*curve B*) shows the asymmetric velocity versus load behavior that results when the basic model is modified asymmetrically by specifying that k_{32} and k_{23} are 0 for $x > 0$. Some of these rate functions are illustrated in Fig. 1 *B*. Although this specification provides an abrupt change in k_{32} at $x = 0$, the results show a much less abrupt change in velocity versus load. In addition, the negative velocities at low values of positive load are greater in magnitude than velocities at high load. Both of these features result because at low loads, x is close to 0, and Brownian motion of the microtubule carries the attached motor back and forth between regions of low and high k_{32}.

When Brownian motion of the microtubule is not included in the computations (results shown by *dashed line C* in Fig. 2), at all positive values of x the detachment rate is 0, and the velocity must be 0. However, for small negative loads, the location of *curve C* in the lower left quadrant means that the microtubule moves to the right, against the imposed load! Therefore, the model is generating work without an energy input—a physical impossibility. When x has a negative value very close to 0, the attachment rate k_{23} is high, $\sim 10^6$ s^{-1} (see Fig. 1 *B*). If Brownian motion is ignored, detachment is likely to be followed by reattachment to the same site after an average time interval of ~ 1 μs. During this time, an applied force of up to 1 pN working against a viscous resistance of 10^{-5} pN s nm^{-1} would move the microtubule no more than 0.1 nm, and reattachment at the same site will be highly favored. However, as seen in Fig. 1 B, attachment to the next site to the right with a strain of $\sim -d$ nm is also possible, but with a lower rate. Because of the asymmetric detachment rate specification, attachment to the next site to the left is not possible as long as x is greater than $-d$, or -8 nm. Consequently, when Brownian motion is ignored, some attachments to the site at $x = +8$ nm will occur, and there will be movement with negative velocity to the right, against the applied load.

This unrealistic movement is eliminated when Brownian motion is included (Fig. 2, *curve B*). When Brownian motion of the microtubule is included, the strain of an attached protein will vary symmetrically about the mean x value close to 0. No detachments will occur when $x > 0$. Detachments when $x < 0$ will occur over a substantial range of values less than 0, rather than just at the value of x close to 0. This range will include values less than $-d$, where detachment can be followed rapidly by attachment at a site to the left, in contrast to the situation without Brownian motion. Cancellation of these effects, to give 0 velocity at 0 load, is expected because both depend upon multiplication of k_{23} by factors that are similar functions of strain. These results clearly demonstrate the importance of making the model realistic by including the effects of thermal fluctuations, or Brownian motion, along the spatial coordinate as well as the effects of thermal fluctuations on the reaction coordinate (Smith, 1998b).

The ability of this asymmetric specification of attachment-detachment equilibrium rates to create a mechanical rectifier at piconewton loads could be quantified, for example, by the ratio between velocities at loads of -1 or $+1$ pN. Attempts to improve this ratio by variation of parameters indicate that there is very little room for improvement. Increasing k_F, or decreasing attachment or detachment rates, gives less rectification. Somewhat better rectification is obtained by reducing the elastic force constant, k_F, but to use low values of k_F without allowing unrealistically high strains, it is necessary to use a nonlinear k_F function that restricts the compliance to a realistic range of distortion values. Computations (not shown) with models containing nonlinear k_F have only slightly improved rectification. Models were also examined with two binding proteins, separated by either 8 or 12 nm. Without other modification, these models have too much resistance in both directions. The resistance can be decreased by reducing the energy difference ΔE_{23} between detached and attached states, but the resulting rectification curves (not shown) are not significantly different from the results shown in Fig. 2.

To explore the maximum capabilities for ratchet performance, the previous results used the most extreme asymmetry in rates, with values of attachment and detachment rates set to 0 for $x > 0$. Results with a less extreme asymmetry, with values of attachment and detachment rates reduced by a factor of 0.01 for $x > 0$, are shown by *curve D* in Fig. 2. As might be expected, this alteration has minimal effect on the results for negative loads, but reduces the resistance to movement with positive loads.

Interaction with asymmetric force functions

Alternatively, asymmetry can be introduced into a model for protein-protein interaction by using different force functions for positive or negative strains. This situation is more complex because Eq. 2 requires that this asymmetry in force functions will also introduce asymmetry in rate functions. As an example, the model illustrated by Fig. 3 was investigated. This model uses a binding site interaction with linear force functions with $k_F = 0.2$ pN nm^{-1} for negative strain and 20 pN nm^{-1} for positive strain. Asymmetry could also be created if each 8-nm substrate repeat contains a

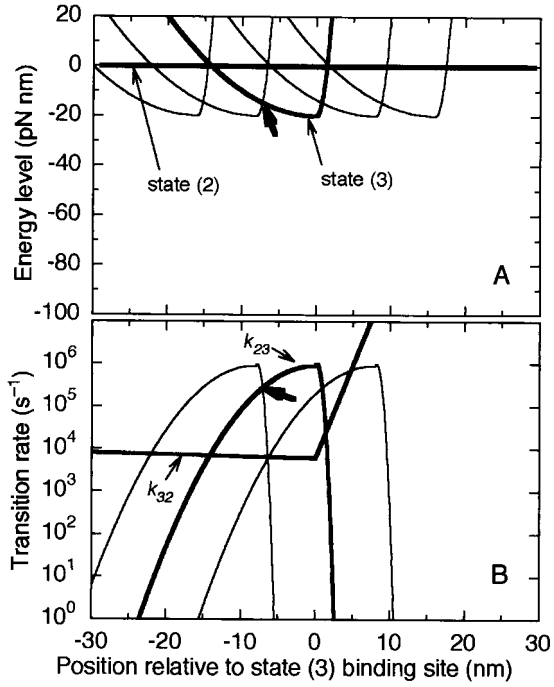

FIGURE 3 *A* shows energy levels for an interaction between a protein and a series of binding sites at 8-nm intervals, with asymmetric compliance. The principal attachment is in state 3, and attachments to two sites on each side are considered; the detached state is state 2. The linear elastic constant for the attached state k_F is 0.2 pN nm^{-1} for negative loads and 20 pN nm^{-1} for positive loads. The effect of this difference in elastic constants on some of the rate functions is illustrated in *B*. For this model, $k_{32}(0) = 6000\ s^{-1}$, $\Delta E_{23} = -20.0$ pN nm, and $a = 0.1$ nm.

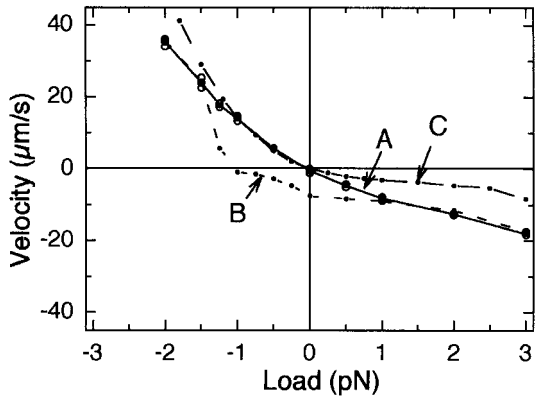

FIGURE 4 *Curves A* and *B* show velocity when a single protein is interacting with sites at 8-nm intervals, as a function of applied load, with the asymmetric elastic constants illustrated in Fig. 3. Brownian motion was included in *A*, but not in *B*. Velocity was averaged over 0.5 s, after a 0.5 startup period to eliminate starting transients. Three computations were performed at each value of load, and shown by *open circles* in *A*. The *solid line* in *A* and the *dashed line* in *B* connect points that are the average of the three computations at each load value. To facilitate comparisons, the *dashed line C* repeats the results shown by *curve D* in Fig. 2, for the weaker version of the asymmetric rate model.

series of closely spaced binding sites with symmetric force functions, with a gradient of binding strength, as illustrated in Fig. 6 *B* of Brokaw (1997). In either case, the result is that to reach a particular level of strain energy, a much greater force magnitude (indicated by the slope of the energy curves in Fig. 3) is required for positive strains than for negative strains.

If a detachment occurs when a negative load and the elastic resistance of the bound protein are in equilibrium at the point where the potential energy curves for the site and the adjacent site intersect (see *bold arrows* in Fig. 3), the rates for reattachment to the same site or to the adjacent site are equal. However, with a positive load of the same magnitude, equilibrium will be reached at a point where attachment to the adjacent site is much less probable than reattachment to the original site. Consequently, transition to adjacent sites will be more frequent with negative loads than with positive loads. This situation reverses for small loads. Near $x = 0$, the probability for a detached molecule to attach to the adjacent site to the left in Fig. 3 is far less than the probability for attachment to the adjacent site to the right. A negative velocity is expected for both positive and negative loads. Computations without Brownian motion confirm this (*dashed line B* in Fig. 4), giving an unrealistic result similar to that obtained when the asymmetric rate model was computed without Brownian motion.

Inclusion of Brownian motion of the microtubule alters this interpretation in two ways. If a molecule detaches near $x = 0$, Brownian motion in the detached state will increase the probabilities for attachment to an adjacent site rather than reattachment to the original site. Because Brownian motion in the detached state is symmetric, when the potential functions are asymmetric, this effect will favor attachment at positive x (negative velocity). This effect has been exploited in the models of Astumian and Bier (1996) and Julicher et al. (1997) by using an energy driven cycle to ensure that detachments occur near $x = 0$. Without such a cycle, the position of detachment is influenced by Brownian motion in the attached state. At 0 load, thermal energy fluctuations of a given magnitude will correspond to much larger values of x in the negative x direction than in the positive x direction. The expected position at 0 load will be at some value of x less than 0, rather than at 0, and this will be the most likely position for detachment to occur. As shown by the complete computation including Brownian motion (*solid line A* in Fig. 4), this effect eliminates the unrealistic negative velocities near 0 load and the result is a rectification curve with realistic properties. This model produces a relatively small asymmetry in velocity, less than was obtained with asymmetry in equilibration rates (Fig. 2). Because this model uses only a 100-fold ratio of force constants, its performance is best compared with that obtained from the model using a 100-fold reduction in rates for $x > 0$ (*curve D* of Fig. 2, which has been reproduced in Fig. 4 as *curve C*).

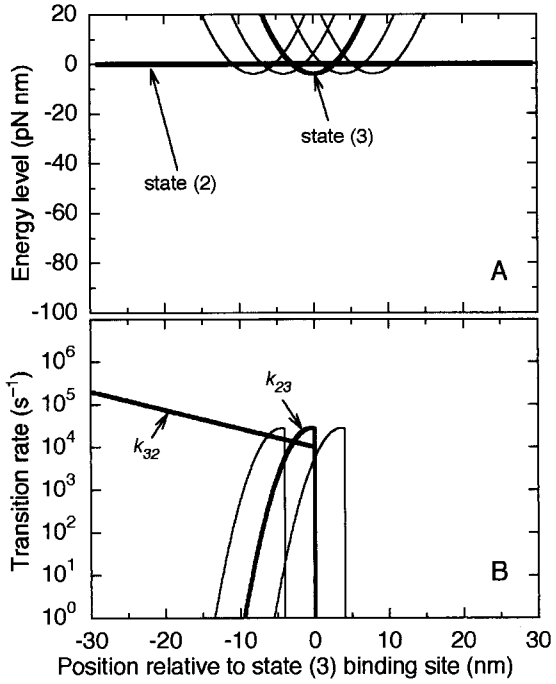

FIGURE 5 Energy levels and rate functions for a model with a less compliant attached state, with sites spaced at 4-nm intervals. This model was used with an ensemble of three proteins spaced at 2.667-nm intervals to obtain the results shown in Figs. 6 and 10. For this model, $k_F = 1.0$ pN nm^{-1}, $k_{32}(0) = 50{,}000$ s^{-1}, $\Delta E_{23} = -4.0$ pN nm, and $a = 1.0$ nm.

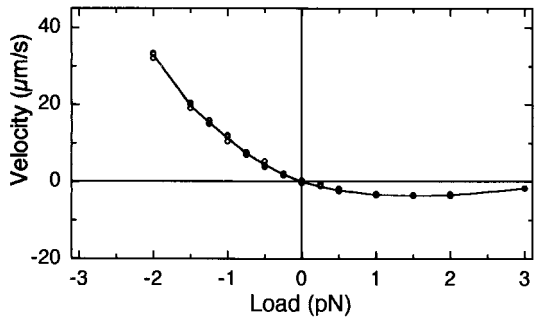

FIGURE 6 Velocity when an ensemble of three proteins is interacting with sites at 4 nm intervals, as illustrated in Fig. 5. Brownian motion was included. Velocity was averaged over 0.5 s, after a 0.5-s startup period to eliminate starting transients. Three computations were performed at each value of load and shown by *open circles*. The *solid line* connects points that are the average of the three computations at each load value.

Ratchets without strain amplification

The previous examples have used a relatively high elastic compliance to ensure that the protein can always reach and bind to a binding site on the substrate. The intrinsic compliance of a binding site interaction will probably limit strain to 1 to 2 nm and require strain amplification to allow an effective strain of 8 nm or more (Brokaw, 1997). Spacing of sites at close intervals (1–2 nm) along the substrate might eliminate the need for strain amplification. A more likely alternative model that uses just the low compliance of the binding site interaction itself can be created by an ensemble of proteins situated so that at least one member of the ensemble is always within range of a binding site on the substrate. This ensemble could also represent multiple binding domains on a single protein. The model illustrated in Fig. 5 uses a site spacing, $d = 4$ nm, with elastic constant $k_F = 1.0$ pN nm^{-1} for the bound protein. An ensemble of three binding proteins spaced at 2.667-nm intervals interacts with these sites. (Similar results, not shown, were obtained with spacing at 1.333-nm intervals.) The possibility of interference between binding proteins must be considered, as detailed in Methods. Fig. 6 shows results obtained with parameters chosen to obtain results comparable with the results in Fig. 2. This model is a less effective rectifier, because with lower compliance the strain values are closer to 0. Consequently, the effects of Brownian motion are proportionately greater, because the root mean square displacement of Brownian motion only decreases as $k_F^{-0.5}$ and the strain values are proportional to k_F^{-1}.

Combining a motor with a protein-protein ratchet

This investigation of ratchet-like behavior of protein-protein interactions was stimulated by reports of processive movement by single-headed motor enzymes (Okada and Hirokawa, 1999; Sakakibara et al., 1999). To enable a single-headed motor to maintain force against a load as it advances to a new site, a second portion of the motor might interact with the substrate to resist backward movement. Ratchet-like behavior might be desirable for this second portion of the motor. In this conception of a processive motor enzyme, the motor enzyme has two independent components. One component is a conventional motor head that executes a mechanochemical cycle using energy from ATP dephosphorylation. The other component is an auxiliary protein-protein interaction of the type discussed in the preceding sections of this paper. The movements of the two components are mechanically coupled by attachment to a common foundation in the cargo end of the motor and interaction with a common substrate microtubule. There is no other interaction between the two components, and, in particular, in this model the ratchet interaction is not incorporated into the mechanochemical cycle of the motor head.

The computer program used by Brokaw (1999) can simulate the behavior of this two-component model because it was designed to model the movement of two parallel ensembles of motors and has the appropriate mechanical coupling between the two ensembles. The program was modified to facilitate the specification of different parameters for each ensemble, as well as by the inclusion of Brownian motion. One ensemble contains a motor enzyme model, and the second ensemble contains the model for protein-protein interaction described in the preceding sections of this paper.

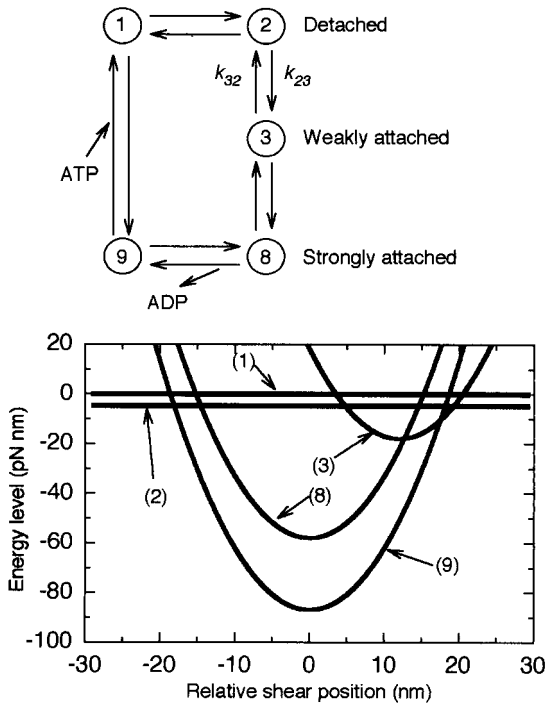

FIGURE 7 A model with a five-state ATPase cycle, used for the motor component of the two-component models. It is a variant of models described in detail in Brokaw; 1999. For clarity, only rates k_{23} and k_{32} are identified, and the additional states required to handle weak attachment to adjacent sites (Fig. 1 *A*) are not shown. The difference between the equilibrium position of state 3, at a relative shear of 12 nm, and the equilibrium position of state 8, at a relative shear of 0 nm, corresponds to a conformational change that drives a power stroke and must be reversed during the strain recovery steps between states 1 and 3. Energy levels relative to state 1 are −5 pN nm for state 2; −18 pN nm at 12 nm shear for state 3; −58 pN nm at 0 shear for state 8; and −87 pN nm at 0 shear for state 9 at 0.5 mM ATP. For computations at 5 μm ATP, ADP concentration is also reduced by a factor of 0.01 and the minimum energy level for state 9 is −105.4 pN nm. The force constant for the attached states is 0.5 pN nm^{-1}. Rate function specifications, in units of s^{-1}, are: k_{12} = 5000; k_{32} = 10,000 at 12 nm shear, increased by load by $\exp(a\,|F(x)|/k_BT)$, with a = 2 nm; k_{38} = 700 for shear ≥ 8 nm, decreasing with a slope of 0.5 $\log_{10}$ units nm^{-1} for shear <8 nm; k_{89} = 900 for shear ≤−5 nm. This value is reduced by a factor of 0.05 for shear > −0.5 nm, with a linear slope between these shear values; k_{91} has the same shear dependence as k_{89}, but its values are determined by setting k_{19} = 6 at 0 shear. In all cases, the reverse rates are determined by the energy difference, as shown for k_{23} in Eq. 2 in the text.

Most computations were performed with only one protein in each ensemble. The motor enzyme model, as described in Brokaw (1999) and Fig. 7, uses a conventional five-state adenosine triphosphatase cycle with a 12-nm power stroke (conformational change). For simplicity, it uses linear force functions, and mechanical detachment from the strongly bound states is not included. The rate constants were adjusted so that at 0.5 mM ATP, an unloaded velocity of 0.8 μm s^{-1} was obtained with a single motor/ratchet pair, and 4.6 μm s^{-1} was obtained with a distributed ensemble of 100 motors and ratchets. These values, indicating a moderately low duty ratio (Howard, 1997), are close to the values of 0.7 μm s^{-1} and 5.1 μm s^{-1} reported by Sakakibara et al. (1999) for inner arm dynein *c*, but the modeling has not taken into account the increased viscosity resulting from inclusion of 0.05% methyl cellulose in these experiments. Velocities with the motor enzyme model alone, without the ratchet interaction, were 1.0 and 5.1 μm s^{-1}, with one or 100 motors, respectively.

Sakakibara et al. (1999) showed that single inner arm dynein *c* motors attached to a bead could move along a stationary microtubule against the load provided by an optical trap and maintain force of 1–2 pN. These experiments were performed at low ATP concentration (5 μM; K. Oiwa, personal communication) where ~6 s was required to move to equilibrium with the load. In the model, reducing ATP concentration to 5 μM and also reducing adenosine 5′-diphosphate (ADP) concentration by a factor of 0.01 reduces the energy level of state 9 and reduces k_{98} and k_{91} by factors of 0.01. As illustrated in Fig. 8 *B*, by itself, this motor enzyme model is unable to maintain significant displacement against an elastic load with a compliance of 0.017 pN nm^{-1}, as used by Sakakibara et al. (1999). However, with an additional protein-protein interaction, identical to that used to obtain the results in Fig. 2 *B*, the two-component model can produce the result shown in Fig. 8 *A*, which is reasonably similar to the result shown in Fig. 4 *C* of Sakakibara et al. (1999). In this case, there is a slow processive movement against the elastic load, reaching equilibrium after ~6 s at ~100 nm, or 1.7 pN. Fig. 8 *C* shows the behavior of the ratchet protein interaction alone under the same conditions. Using a symmetric version of the additional protein-protein interaction, without reducing k_{32} to 0 for $x > 0$, eliminates the ability of the complex to move against a load (Fig. 9 *A*), with a result very similar to that obtained for the motor domain alone (Fig. 8 *B*). Fig. 9 *B* shows results with a reversed ratchet, with $k_{32} = 0$ for $x < 0$. There is a small shift in average position, resulting from the drag of the protein interaction in both directions, but the effect is much less than in Fig. 8 *A*. Fig. 10 shows that similar results can be obtained when the auxiliary protein-protein interaction component is replaced with the lower compliance model of Fig. 5, which uses three interacting proteins in the ratchet. These results demonstrate that a ratchet-like protein-protein interaction can usefully complement the operation of a single motor enzyme.

Replacing the auxiliary protein-protein interaction component with the model of Fig. 2 *D*, which has only a 100-fold reduction in rates for $x > 0$, also gives a two-component model that can move effectively against a load (Fig. 11 *A*). Similar results (not shown) can also be obtained simply by increasing the viscous load on the bead from 10^{-5} to 3×10^{-4} pN nm s^{-1}, but, at this viscosity level, the movement at 0.5 mM ATP is reduced to only 2.5 μm s^{-1}. This resembles an earlier calculation by Chen (2000), indicating that a single one-headed kinesin motor could move a

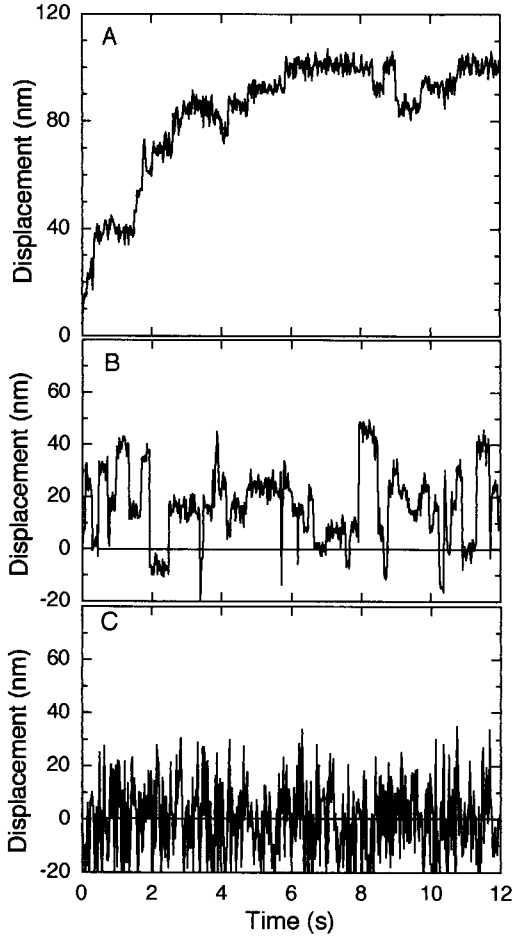

FIGURE 8 *A* shows movement generated against an elastic load of 0.17 pN nm^{-1} by a combination of a motor enzyme model, specified in Fig. 7, and the protein ratchet of Figs. 1 and 2 *B*. Computed with 10^{-7} s time steps and sampled at 24-ms intervals. Movement generated against an elastic load of 0.17 pN nm^{-1} by the motor enzyme model alone is shown in *B*, and movement of the protein ratchet alone is shown in *C*.

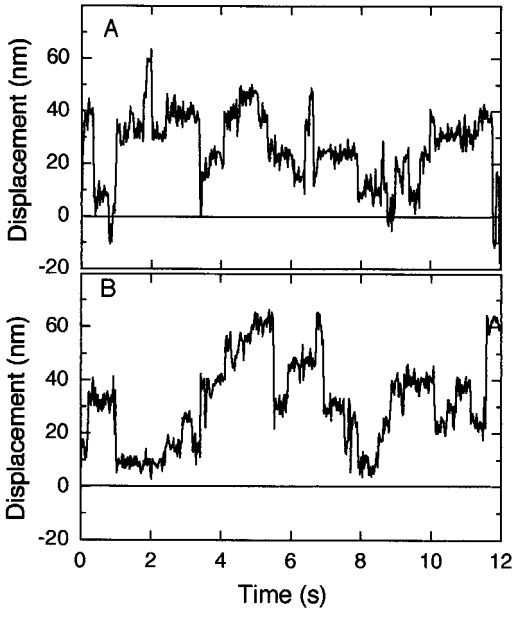

FIGURE 9 Additional results for movement generated against an elastic load of 0.17 pN nm^{-1} by variants of the model used for Fig. 8 *A*. In *A*, the ratchet is replaced with the symmetric protein interaction used for Fig. 2 *A*. In *B*, the direction of the ratchet is reversed, by specifying that the rates are 0 for $x < 0$.

bead slowly against a load of 0.8 pN if a 100-fold increase in viscosity was used to retard backward slippage when the kinesin head is detached. Although replacing the auxiliary protein-protein interaction component with the symmetric protein-protein interaction model of Fig. 2 *A* did not support movement against a load (Fig. 9 *A*), the result with increased viscous resistance suggests that models containing symmetric protein-protein interaction components with greater resistance should be examined. Fig. 11 *B* shows results with the symmetric model for the protein-protein interaction component, after its resistance was increased by reducing $k_{32}(0)$ from 10,000 to 1000 s^{-1} and increasing the magnitude of ΔE_{23} from -20 pN nm to -40 pN nm. The resistance of this binding interaction permits movement that is slightly better than that obtained with the motor enzyme model alone (Fig. 8 *B*), but significantly less than that obtained with the ratchet interactions (Figs. 8 *A*, 10 *A*, or 11 *A*). Although this interaction is not sufficient to give good interaction against a load, it significantly decreases the movement of an ensemble of 100 motor/binding protein pairs at 0.5 mM ATP from 4.6 μm s^{-1} to 3.5 μm s^{-1}. With a further decrease in $k_{32}(0)$ to 300 s^{-1}, the movement against a load was still significantly below that obtained with the ratchet interactions, and the movement velocity at 0.5 mM ATP was further reduced to 2.4 μm s^{-1} (not shown).

These results confirm the idea that addition of an accessory protein-protein interaction component can prevent backward slippage and enable a single motor enzyme to move processively against a load. They also support the idea that a ratchet interaction is a desirable feature of this accessory protein-protein interaction, to prevent excessive resistance to forward movement. Since the results with symmetric interactions begin to provide an ability for processive movement against a load, they suggest that even a weaker ratchet interaction than that obtained with the model of Fig. 2 *D* may be sufficient to obtain results similar to those observed in the experiments with inner arm dynein *c*. However, the asymmetric force function model of Fig. 3, which has a very weak ratchet effect, did not provide adequate load-bearing capability (Fig. 11 *C*), although the resistance of this model reduces the movement velocity with 100 motor/ratchet pairs at 0.5 mm ATP to 3.4 μm s^{-1}.

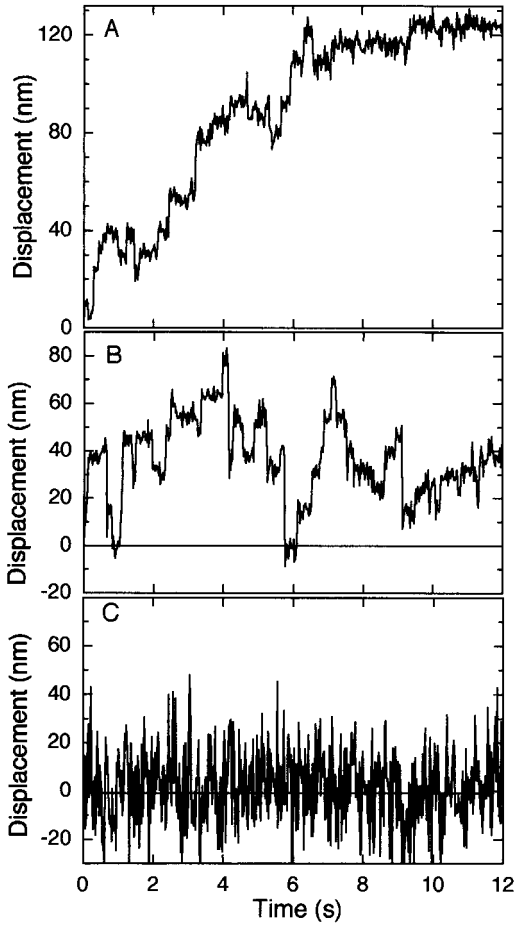

FIGURE 10 *A* shows movement generated against an elastic load of 0.17 pN nm^{-1} by a combination of a motor enzyme model, specified in Fig. 7, and the three-element protein ratchet of Figs. 5 and 6. At high ATP concentration (0.5 mM), this combination gives a velocity of 1.3 $\mu m\ s^{-1}$ with one motor/ratchet pair and 4.9 $\mu m\ s^{-1}$ with a distributed ensemble of 100 motors and ratchets. Computed with 10^{-7} s time steps and sampled at 24-ms intervals. Movement generated against the elastic load when the direction of the ratchet is reversed is shown in *B*, and movement of the protein ratchet alone is shown in *C*.

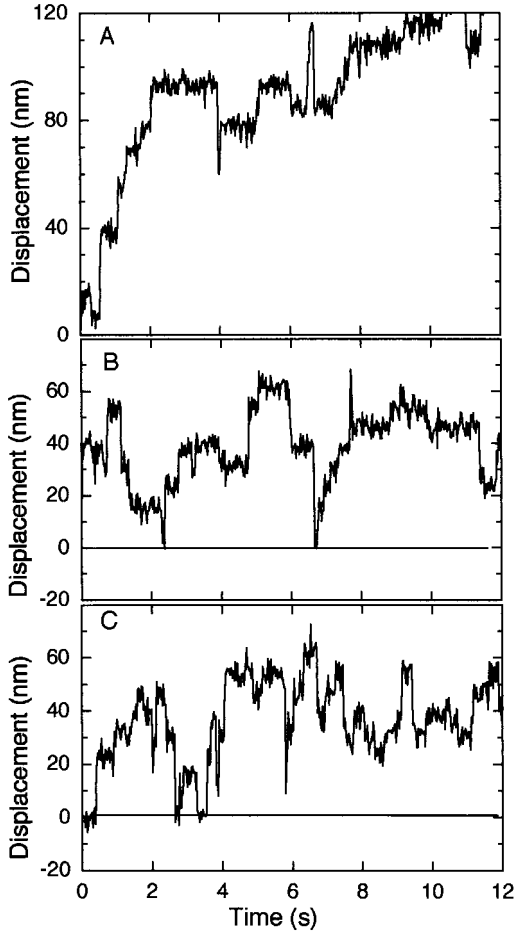

FIGURE 11 Movement generated against an elastic load of 0.17 pN nm^{-1} by a combination of a motor enzyme model, specified in Fig. 7, and accessory protein interactions. In *A* the accessory protein interaction is the weaker version of the asymmetric rate model, as illustrated by the results in *curve D* of Fig. 2, with k_{32} reduced by a factor of 0.01 for $x > 0$. In *B*, the accessory protein interaction is symmetric, as in Fig. 2 *A*, but the parameters have been changed to provide a greater resistance, by setting $k_{32}(0) = 1000\ s^{-1}$ and $\Delta E_{23} = -40$ pN nm. In *C* the accessory protein interaction is the model used for Fig. 6, with asymmetric force constants, as shown in Fig. 5. Computed with 10^{-7} s time steps and sampled at 24-ms intervals.

DISCUSSION

Simulations of molecular ratchets

Within the realm of mathematical models, it is easy to introduce spatial asymmetry into the specification of a binding interaction between proteins and compute the resulting behavior using stochastic simulations. These simulations indicate that asymmetry in attachment and detachment rates is an effective means to obtain ratchet-like behavior of the binding interaction. Introduction of asymmetric compliance, by specifying different force constants for positive or negative displacements, is much less effective.

The computations of ratchet interactions show clearly the importance of thermal fluctuations, which limit the effectiveness of a ratchet in the piconewton and nanometer range. Modeling experiments with single molecules emphasize the degree of freedom for thermal fluctuations that cause Brownian motion of either the microtubule or the bead, depending upon the experimental situation. However, even in situations where this type of Brownian motion is greatly reduced, perhaps by a large increase in stiffness resulting from multiple attachments with a large ensemble of interacting molecules, thermal fluctuations will occur internally within each interacting molecule. At a minimum, there will be fluctuations in the force associated with the compliance of each binding interaction, and there may be additional fluctuations associated with other internal degrees of freedom of the molecules. The effect of Brownian motion modeled here represents the least possible effect of thermal

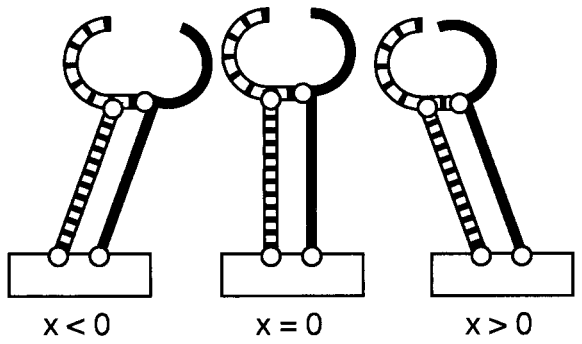

FIGURE 12 Cartoon of a mechanical device that opens and closes a pocket as a function of tilt, to indicate how access to a binding site might be determined by strain. Three rigid links, distinguished by shading, are attached together and to a solid base at four pivot points (*small circles*). The central image represents the 0 strain condition corresponding to $x = 0$.

fluctuations. In real molecules there may well be additional effects of thermal fluctuations that make it difficult to achieve even the modest ratchet performance at the piconewton and nanometer range found with these models.

These ratchets are not, by themselves, molecular motors that generate unidirectional motion by using chemical energy to capture thermal fluctuations in one direction. Such "Brownian ratchet" motors work by exploiting thermal fluctuations; in contrast, the ratchet interactions discussed in the present paper work despite thermal fluctuations.

Molecular implementations

Can actual molecular interactions generate the asymmetry that is required for an effective ratchet? Molecular mechanisms that provide for asymmetric compliance are easy to imagine, but the simulation results (Figs. 4 and 11 *C*) suggest that asymmetric compliance does not generate a useful ratchet. A useful ratchet can be created by introducing strain dependence of the attachment and detachment rate functions, as depicted in Fig. 1 *B*, but is this realistic at the molecular level? This type of abrupt strain dependence was introduced in the $g(x)$ function for the detachment rate of strongly bound cross-bridges in the Huxley (1957) model for myosin-actin interaction in skeletal muscle. A specific molecular model for myosin-actin interaction involving strain-dependent opening and closing of a nucleotide-binding pocket was described by Smith and Geeves (1995). These authors recognized that thermal fluctuations would influence the opening and closing of this pocket, and they incorporated the effect of thermal fluctuations into their specifications of strain-dependent reaction rates. A different type of molecular model is needed for strain dependence of the binding and unbinding reactions of the ratchet models considered here (Fig. 1), because these reactions do not depend upon nucleotide binding.

Fig. 12 is a cartoon representation of a mechanical device involving opening and closing of a pocket, which could provide the strain dependent attachment and detachment rates used for the ratchet model. The elastic strain resistance could be incorporated into the hinges, or could reside in accessory components coupled to the bending motion of this device. To obtain an abrupt restriction of attachment and detachment at $x > 0$, the components of this device must be completely rigid, except for the four hinges, and the attachment and detachment reactions must be completely dependent upon opening the pocket to a gap wider than that shown for $x = 0$. Any internal compliance would make opening and closing of the pocket partially independent of strain and introduce another degree of freedom for thermal fluctuations, decreasing the abruptness of the strain dependence of attachment and detachment rates. The results shown in Fig. 2 *B* represent an ideal model that can only be approximated by a real molecular implementation, and the structural requirements for a molecular implementation are considerable.

To have only very short periods of detachment when sites are spaced at 8 nm intervals, a protein must be sufficiently compliant to allow the attached state to be stable over distances of the order of ± 8 nm. Since the intrinsic forces of binding interaction typically act over strains of no more than 1 to 2 nm, this compliance requires some form of strain amplification, as previously discussed for motor enzymes (Brokaw, 1997). The mechanism cartooned in Fig. 12 provides for strain amplification by a lever arm, which is a common assumption for myosin and kinesin motor function. Because there is no structural evidence for a second lever arm domain that could function in this manner to assist the processive movement of a single-headed motor, there is reason to consider alternatives that do not require strain amplification by a lever arm.

There are at least two possible alternatives. One assumes short-range binding interaction, over distances of less than $\sim \pm 2$ nm, with asymmetric rate functions, and ensures continuous attachment by having multiple binding regions, so that at least one is always within range of a binding site on the substrate (Fig. 5). The simulation results in Fig. 6 indicate that this model creates a somewhat less satisfactory ratchet, because the effects of thermal fluctuations become more significant as the spatial scale of the model is reduced. The smaller spatial scale involved in these interactions might also increase the difficulty of incorporating the requisite structural asymmetry into the binding site interactions. The other alternative assumes short-range binding interaction with symmetric rate functions, and uses a series of sites with graded affinities to produce an asymmetric strain amplification (Brokaw, 1997). This possibility has been approximated here by using asymmetric force constants (Fig. 3). The computations show that this construction does not give a very useful ratchet (Figs. 4, 11 *C*).

Ratchets as components of processive enzymes

Processive enzymes step from site to site along a substrate polymer, in conjunction with a biochemical cycle that is executed at each step. Processive movement became well known after visual observations demonstrated the continuous movement of microtubules by single molecules of the motor enzyme kinesin (Howard et al., 1989). Conventional kinesin is a homodimer with two motor domain "heads." Various models have been proposed that successfully explain the processive movement of two-headed motor enzymes by a coordinated "hand over hand" stepping of the two heads (Peskin and Oster, 1996; Duke and Leibler, 1996; Rice et al., 1999; Brokaw, 2000). More recently, processive movement has been recognized as a property of RNA polymerase (Gelles and Landick, 1998) and single-headed motor enzymes such as kinesin superfamily member KIF1A (Okada and Hirokawa, 1999) and inner arm dynein *c* (Sakakibara et al., 1999). In some of these cases, the ability of single molecules to move and maintain position against a load imposed by an optical trap has been demonstrated. In the simplest models, a motor enzyme moving against a load might be expected to be pushed backwards when it releases its attachment to one substrate site to attach to another substrate site. An auxiliary interaction between the motor enzyme and its substrate, separate from the primary interaction of the motor enzyme with substrate sites, has been suggested as a mechanism to prevent backward movement (Okada and Hirokawa, 1999; Sakakibara et al., 1999). In the case of KIF1A, in addition to the primary microtubule-binding interaction, there is a lysine-rich "K-loop" that is a good candidate for an auxiliary interaction with a glutamate-rich region near the C-terminus of tubulin (Okada and Hirokawa, 1999).

A key idea in this modeling is that the motor enzyme interaction and the ratchet-like protein-binding interaction are independent. The assistance provided by the auxiliary protein-binding interaction does not require the type of coordination that has been proposed for dimeric motors such as conventional kinesin. The results presented demonstrate that, for a particular motor enzyme model, an auxiliary protein-binding interaction can prevent backward movement by an external load, but it will significantly restrict the ability of the motor enzyme to produce rapid movement at higher ATP concentrations unless the auxiliary interaction has ratchet-like properties. The requisite ratchet-like properties seem to require a binding interaction with asymmetric strain dependency of the attachment and detachment rates, and molecular implementation of this interaction may be structurally complex. This result cannot be generalized to all possible motor enzyme models, which comprise a large universe. There may be motor enzyme models for which a simpler auxiliary interaction, without asymmetry, may be sufficient to prevent backward movement under load without seriously restricting the ability of the motor enzyme to generate forward movement.

Modeling inner arm dyneins

These modeling results, such as Fig. 8 *A*, support previous suggestions that an auxiliary binding interaction may explain the ability of single molecules of inner arm dynein *c* to move processively against a load provided by an optical trap in the experiments of Sakakibara et al. (1999). By adjusting parameters of the motor enzyme model, it was possible to obtain velocities for 1 or 100 motor/ratchet pairs at 0.5 mM ATP similar to the results reported by Sakakibara et al. (1999), indicating that the resistance of the ratchet in its permissive direction is sufficiently low at these realistic velocities. After adjusting the model for 5 μM ATP, it was possible to reproduce the velocity and equilibrium load obtained by Sakakibara et al. (1999) for single motors moving against the load of an optical trap. However, no attempt has been made here to provide a complete model for inner arm dynein *c* that explains all the interesting features of these experimental results. In particular, the results indicate that the stiffness of the attached dynein increases with increasing loads. This feature could probably be reproduced by a model that uses a nonlinear elastic function for the binding interaction. The results of Sakakibara et al. (1999) also show occasional detachments, during which the bead moves rapidly toward its equilibrium position before the dynein reattaches and again moves against the load provided by the optical trap. In the models used here, the attachment probabilities for either the motor enzyme component or the ratchet protein component are independent of the state of the other component. More realistically, the probability of making an attachment from a "both detached" state is likely to be less than from a state in which only one of the components is detached. In this manner, there is likely to be cooperativity between the two components. A more complicated model that considers cooperativity between the two components, as in a model used for two-headed motor enzymes (Brokaw, 2000), is needed to provide a complete interpretation of the behavior of inner arm dynein *c*.

Although a ratchet interaction would seem to be useful for explaining the in vitro observations with inner arm dynein *c*, the functioning of inner arm dynein *c* within an axoneme is a different situation. Within an axoneme, dyneins encounter back and forth sliding during each flagellar beat cycle, and a ratchet interaction that impedes backward movement might be undesirable, unless there is a control mechanism that completely prevents interaction of the dynein with the substrate microtubule during the backward portion of the cycle. This type of control mechanism may be required in any event, to turn off dynein driven movement during half the beat cycle. Our present understanding of dynein function within an axoneme is too primitive to

explain why processivity would be an advantageous capability for axonemal dyneins.

REFERENCES

Astumian, R. D., and M. Bier. 1996. Mechanochemical coupling of the motion of molecular motors to ATP hydrolysis. *Biophys. J.* 70:637–653.

Brokaw, C. J. 1976. Computer simulation of movement–generating cross-bridges. *Biophys. J.* 16:1013–1027.

Brokaw, C. J. 1995. Weakly-coupled models for motor enzyme function. *J. Muscle Res. Cell Mot.* 16:197–211.

Brokaw, C. J. 1997. Mechanical components of motor enzyme function. *Biophys. J.* 73:938–951.

Brokaw, C. J. 1999. Computer simulation of flagellar movement: VII. Conventional but functionally different cross-bridge models for inner and outer arm dyneins can explain the effects of outer arm dynein removal. *Cell Motil. Cytoskel.* 42:134–148.

Brokaw, C. J. 2000. Stochastic simulation of processive and oscillatory sliding using a two-headed model for axonemal dynein. *Cell Motil. Cytoskel.* 47:108–119.

Chen, Y. 2000. Theoretical formalism for kinesin motility I. Bead movement powered by single one-headed kinesins. *Biophys. J.* 78:313–321.

Cordova, N. J., B. Ermentrout, and G. F. Oster. 1992. Dynamics of single-motor molecules: the thermal ratchet model. *Proc. Natl. Acad. Sci. U.S.A.* 89:339–343.

Duke, T., and S. Leibler. 1996. Motor protein mechanics: a stochastic model with minimal mechanochemical coupling. *Biophys. J.* 71: 1235–1247.

Feynman, R., R. B. Leighton, and M. Sands. 1966. The Feynman Lectures on Physics, Vol. 1. Addison-Wesley, Reading MA, A6-1–A6-9.

Gelles, J., and R. Landick. 1998. RNA polymerase as a molecular motor. *Cell.* 93:13–16.

Hill, T. L. 1974. Theoretical formalism for the sliding filament model of contraction of striated muscle. Part I. *Prog. Biophys. Mol. Biol.* 28: 267–340.

Howard, J. 1997. Molecular motors: structural adaptations to cellular functions. *Nature.* 389:561–567.

Howard, J., A. J. Hudspeth, and R. D. Vale. 1989. Movement of microtubules by single kinesin molecules. *Nature.* 342:154–158.

Huxley, A. 1957. Muscle structure and theories of contraction. *Prog. Biophys.* 7:255–318.

Julicher, F., A. Ajdari, and J. Prost. 1997. Modeling molecular motors. *Rev. Modern Physics.* 69:1269–1281.

Keller, D., and C. Bustamente. 2000. The mechanochemistry of molecular motors. *Biophys. J.* 78:541–556.

Kagami, O., and R. Kamiya. 1992. Translocation and rotation of microtubules caused by multiple species of *Chlamydomonas* inner-arm dynein. *J. Cell Sci.* 103:653–664.

Nishizaka, T., R. Seo, H. Tadakuma, K. Kinosita, Jr., and S. Ishiwata. 2000. Characterization of single actomyosin rigor bonds: load dependence of lifetime and mechanical properties. *Biophys. J.* 79:962–974.

Okada, Y., and N. Hirokawa. 1999. A processive single–headed motor: kinesin superfamily protein KIF1A. *Science.* 283:1152–1157.

Pate, E., and R. Cooke. 1991. Simulation of stochastic processes in motile crossbridge systems. *J. Musc. Res. Cell Motil.* 12:376–393.

Peskin, C. S., and G. Oster. 1996. Coordinated hydrolysis explains the mechanical behavior of kinesin. *Biophys. J.* 68:202s–211s.

Press, W. H., B. P. Flannery, S. A. Teikolsky, and W. T. Vetterling. 1986. Numerical Recipes. Cambridge Univ. Press, Cambridge, U.K.

Rice, S., A. W. Lin, D. Safer, C. L. Hart, N. Naber, B. O. Carragher, S. M. Cain, E. Pechatnikova, E. M. Wilson-Kubalek, M. Whittaker, E. Pate, R. Cooke, E. W. Taylor, R. A. Milligan, and R. D. Vale. 1999. A structural change in the kinesin motor protein that drives motility. *Nature.* 402: 778–784.

Sakakibara, H., H. Kojima, Y. Sakai, E. Katayama, and K. Oiwa. 1999. Inner arm dynein *c* of *Chlamydomonas* flagella is a single-headed processive motor. *Nature.* 400:586–590.

Schoenberg, M. 1985. Equilibrium muscle cross-bridge behavior. *Biophys. J.* 48:467–475.

Smith, D. A. 1998a. A strain-dependent ratchet model for [phosphate]-and [ATP]-dependent muscle contraction. *J. Muscle Res. Cell Motil.* 19: 189–211.

Smith, D. A. 1998b. Direct tests of muscle cross-bridge theories: Predictions of a Brownian dumbbell model for position-dependent cross-bridge lifetimes and step sizes with an optically trapped actin filament. *Biophys. J.* 75:2996–3007.

Smith, D. A., and M. A. Geeves. 1995. Strain-dependent crossbridge cycle for muscle. *Biophys. J.* 69:524–537.

Strunz, T., K. Oroszlan, I. Schumakovitch, H. Guntherodt, and M. Hegner. 2000. Model energy landscapes and the force-induced dissociation of ligand-receptor bonds. *Biophys. J.* 79:1206–1212.

Tawada, K., and K. Sekimoto. 1991. Protein friction exerted by motor enzymes through a weak-binding interaction. *J. Theor. Biol.* 150: 193–200.

Vale, R. D., and Y. Y. Toyoshima. 1988. Rotation and translocation of microtubules in vitro induced by dyneins from *Tetrahymena* cilia. *Cell.* 52:459–469.

Vale, R. D., and F. Oosawa. 1990. Protein motors and Maxwell's demons: does mechanochemical transduction involve a thermal ratchet? *Adv. Biophys.* 26:97–134.